



HAL
open science

High-valence Cu^ICu^{III} species in action: demonstration of aliphatic C–H bond activation at room temperature

James Alfred Isaac, Aurore Thibon-Pourret, Amélie Durand, Christian Philouze, Nicolas Le Poul, Catherine Belle

► To cite this version:

James Alfred Isaac, Aurore Thibon-Pourret, Amélie Durand, Christian Philouze, Nicolas Le Poul, et al.. High-valence Cu^ICu^{III} species in action: demonstration of aliphatic C–H bond activation at room temperature. *Chemical Communications*, Royal Society of Chemistry, 2019, 55 (84), pp.12711-12714. 10.1039/C9CC04422A . hal-02308483

HAL Id: hal-02308483

<https://hal.univ-grenoble-alpes.fr/hal-02308483>

Submitted on 23 Oct 2020

HAL is a multi-disciplinary open access archive for the deposit and dissemination of scientific research documents, whether they are published or not. The documents may come from teaching and research institutions in France or abroad, or from public or private research centers.

L'archive ouverte pluridisciplinaire **HAL**, est destinée au dépôt et à la diffusion de documents scientifiques de niveau recherche, publiés ou non, émanant des établissements d'enseignement et de recherche français ou étrangers, des laboratoires publics ou privés.

High-valent Cu^{II}Cu^{III} Species in Action: Demonstration of Aliphatic C–H Bond Activation at Room Temperature

James A. Isaac,^a Aurore Thibon-Pourret,^{*a} Amélie Durand,^b Christian Philouze,^a Nicolas Le Poul^{*c} and Catherine Belle^{*a}

Abstract: The electrochemically generated Cu^{II}Cu^{III} mixed-valent species promotes activation of strong aliphatic C–H bond (i.e. toluene) at room temperature. The mechanistic pathway turns from stoichiometric to catalytic upon addition of base, hence demonstrating that such high-valent dicopper species can be key reactive intermediates in copper-based oxidative processes.

Mild, efficient and direct routes for C–H oxidation/oxygenation to form industrially valuable products is of considerable interest in addressing mild and sustainable synthetic procedures and current energy concerns.¹ In this context, copper-based catalysts appear as good alternatives to precious metal because of its natural abundance, low toxicity and low-cost nature. Hence, various copper-based catalysts have been developed using O₂ as terminal oxidant.² Biomimetic approaches have proven to be very helpful by elucidating the nature of oxido, hydroxido, peroxido or superoxido copper intermediates able to mediate C–H bond activation. Each of them displays distinct abilities for oxidation-oxygenation including cross coupling reactions as described in several reviews.³ Among them Cu^{II}Cu^{III} mixed-valent species have been previously suggested as possible intermediates for C–H bond activation.^{3f, 4} Challenges remain to explore the capability of such species in oxidation as examples are scarce⁵ and only one^{5a} demonstrated C–H bond activation on a fairly weak bond (i.e. dihydroanthracene).

Dipyridylethane naphthyridine (L) and its analogs act as compartmental ligands and have allowed the isolation of dinuclear complexes with metallic centers in close proximity.⁶ Recently, from L as bridging ligand, we have prepared the dinuclear copper(II) complex **1** ([Cu^{II}₂(L)(μ-OH)₂(OTf)](OTf) where OTf = CF₃SO₃⁻).⁷ Because of the presence of a triflate anion at one copper site, the two Cu atoms are not in identical

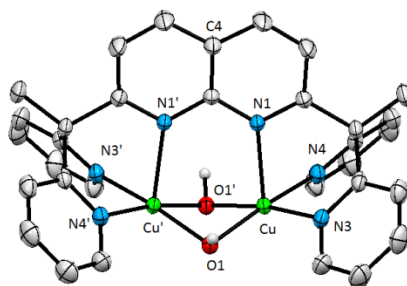


Fig. 1 ORTEP of the cationic part of [Cu^{II}₂(L)(μ-OH)₂](ClO₄)₂·6H₂O (2·6H₂O)(50% probability ellipsoids). H atoms (except from the OH) have been omitted. See ESI for details

coordination environments at solid state: one copper displays a distorted square pyramidal geometry and the other is found in a distorted octahedral geometry. Based on UV-Vis-NIR, EPR data and theoretical calculations, electrochemical mono-electronic oxidation of **1** in CH₃CN promotes formation of the corresponding mixed-valent Cu^{II}Cu^{III} species⁷ assigned to a class II in the Robin-Day classification at room temperature.⁸ The data suggest that the hydroxido bridges remain coordinated and protonated after the mono-oxidation into **1**⁺.

We have initiated our studies by probing the behavior of the starting complex **1** in the presence of an excess of ClO₄⁻ since our voltammetric studies have been carried out in NBu₄ClO₄/CH₃CN. After slow evaporation, crystals of [Cu^{II}₂(L)(μ-OH)₂](ClO₄)₂·6H₂O (**2**·6H₂O) suitable for X-ray analysis (details in ESI) were obtained, hence evidencing the removal of the triflate anion in the copper coordination sphere. The symmetrical entity **2** obtained (Fig. 1) displayed similar metrical parameters to those of **1** (Table S1) with a slightly longer Cu...Cu distance (2.793 Å vs. 2.751 Å in **1**) and both Cu atoms in square pyramidal geometry. This result suggested that **1** and **2** are equivalent upon dissolution into acetonitrile in presence of ClO₄⁻. To explore the capability of **1**⁺ to perform C–H activation, we have taken advantage of an electrochemical approach as a more environmentally friendly solution⁹ avoiding stoichiometric chemical oxidants.¹⁰

^a Université Grenoble Alpes, CNRS, DCM, 38000 Grenoble, France.

E-mail: catherine.belle@univ-grenoble-alpes.fr

^b Université Grenoble Alpes, CNRS, ICMG, 38000 Grenoble, France

^c Université de Bretagne Occidentale, CNRS UMR 6521, 6 Avenue Le Gorgeu, CS 93837, 29238 Brest, France. E-mail: nicolas.lepoul@univ-brest.fr

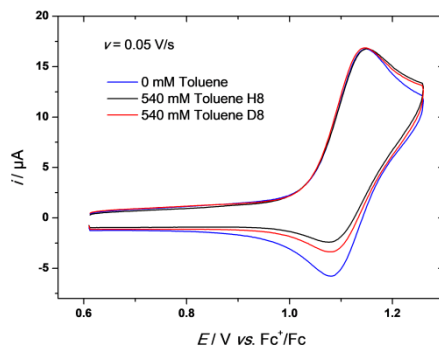


Fig. 2 CVs of **1** (1.2 mM) upon the addition of toluene-H8 (black) or toluene-D8 (red); 0.1 M $\text{NBu}_4\text{ClO}_4/\text{CH}_3\text{CN}$ at 20°C under Ar.

So far, copper-based electrochemical studies have been restrained to water oxidation or oxygen/ CO_2 reduction¹¹ and this strategy has not been explored for the catalytic oxidation of strong C–H bonds by copper species. We then focused our studies on the oxidation of toluene (Bond dissociation energy (BDE) = 89.8 kcal·mol⁻¹)¹² by the electrochemically generated complex **1**⁺. The direct oxidation of the aliphatic C–H bond in toluene is faced by several drawbacks such as high temperatures and pressures and by-products.¹³ Rare examples have been reported from bio-inspired models involving Cu_2/O_2 intermediates¹⁴ possibly in confined environment.¹⁵ Furthermore, to date, catalytic turnover is still regarded as a challenge.

Cyclic voltammetry (CV) of the dicopper(II) complex **1** in $\text{NBu}_4\text{ClO}_4/\text{CH}_3\text{CN}$ is shown in Fig. 2 (blue curve). The complex exhibits a quasi-reversible system at $E_{1/2}(\mathbf{1}) = 1.12$ V vs. Fc^+/Fc which can be ascribed to the $\mathbf{1} \rightarrow \mathbf{1}^+$ reaction from our previous studies.⁷ At very low scan rate (0.02 V·s⁻¹, Fig. S2), the cathodic to anodic peak current ratio (i_{pc}/i_{pa}) decreases due to the probable reaction of the oxidized species with the solvent, as reported.⁷ As shown in Fig. 2, S2 and S3, a significant loss of reversibility was observed upon addition of toluene-H8 (110 to 500 mol. equiv.), within the studied scan-rate range (0.02 V·s⁻¹ < ν < 0.2 V·s⁻¹). This result suggested us that the $\text{Cu}^{\text{II}}\text{Cu}^{\text{III}}$ species **1**⁺ reacts with that substrate. Experiments performed with toluene-D8 also led to a decrease of the cathodic peak current but in a less pronounced manner (Fig. 2), indicating a kinetic isotope effect (KIE). Voltammetric simulation of the CVs allowed the determination of the forward rate constant, k_f , for the chemical oxidation of toluene by **1**⁺ (details in ESI, Scheme S1 and Figs S2-S3). The experimental behavior was reproduced for different values of substrate concentration and different scan rates. We found that $k_f = 1.1 \text{ M}^{-1}\cdot\text{s}^{-1}$ and $0.5 \text{ M}^{-1}\cdot\text{s}^{-1}$, for H8- and D8-toluene, respectively, yielding a KIE value $k_f(\text{H})/k_f(\text{D}) = 2.2$. It indicates that the rate determining step (RDS) involves cleavage of the C–H bond of the substrate upon electrochemical oxidation of **1**. However, the reaction remains stoichiometric and not catalytic, as shown by the comparable anodic peak current $i_{pa}(\mathbf{1})$ values obtained in absence and presence of toluene (Fig. S4).

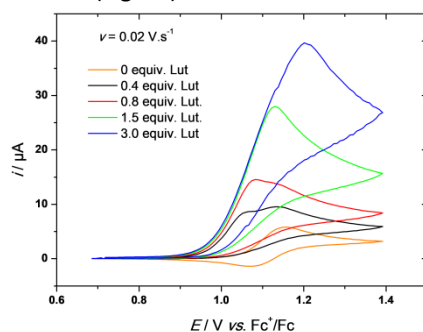


Fig. 3 CVs of complex **1** (0.8 mM) upon addition of 2,6-lutidine (Lut). 0.1 M $\text{NBu}_4\text{ClO}_4/\text{CH}_3\text{CN}$; [Lut] = 0.3, 0.6, 1.2 and 2.4 mM at 20°C under Ar.

Electrolysis of **1** in $\text{NBu}_4\text{ClO}_4/\text{CH}_3\text{CN}$ with toluene in excess (490 equiv.) followed by purification and analysis by GC-MS (see ESI, Fig. S5) allowed the oxidation products of toluene to be determined. Among them, benzaldehyde, benzyl alcohol, benzylacetamide, 2-(methylphenyl)-toluene and 4-(methylphenyl)-toluene were detected, consistent with a radical processes involving Ph-CH_2^\bullet formation, recombination or attack at nitrogen on the solvent.¹⁶ In order to determine the possible O atom source, an exhaustive electrolysis of **1** was performed in a solution of $\text{NBu}_4\text{ClO}_4/\text{CH}_3\text{CN}$ containing H_2^{18}O under argon (details in ESI, Fig. S6 and Table S2). Analysis by GC-MS evidenced that ¹⁸O from added water was incorporated into benzyl alcohol, benzaldehyde and benzylacetamide

along with non-labelled O atom, hence suggesting that oxygen atom transfer may also involve others sources (hydroxido bridge or residual water).

Having demonstrated that the $\text{Cu}^{\text{II}}\text{Cu}^{\text{III}}$ species is reactive towards the strong aliphatic C–H bond of toluene, we then focused our efforts on making the system catalytic. Presumably, the reaction of $\mathbf{1}^+$ with toluene leads to the formation of an inactive $(\mu\text{-OH})(\text{OH}_2)\text{Cu}^{\text{II}}\text{Cu}^{\text{II}}$ species through a proton-coupled electron transfer (PCET). Investigations were therefore carried out using 2,6-lutidine(Lut) with the aim of regenerating the bis($\mu\text{-OH}$) $\text{Cu}^{\text{II}}\text{Cu}^{\text{III}}$ core from the $(\mu\text{-OH})(\text{OH}_2)\text{Cu}^{\text{II}}\text{Cu}^{\text{II}}$ adduct. First studies were performed in absence of toluene in order to investigate the oxidative properties of the species resulting from the oxidation and deprotonation of $\mathbf{1}$. CVs of $\mathbf{1}$ in $\text{NBu}_4\text{ClO}_4/\text{CH}_3\text{CN}$ upon addition of 2,6-lutidine are displayed in Fig. 3. A dramatic rise in the current was observed with increasing the concentration in Lut, symptomatic of an electrocatalytic wave. A pre-peak was detected at ca. $E_{\text{pa}}(2) = 1.05$ V vs. Fc^+/Fc for sub-stoichiometric amounts of Lut. The potential of the pre-peak increased upon further addition of Lut, whereas the potential of the second peak at $E_{\text{pa}}(1) = 1.15$ V vs. Fc^+/Fc assigned to the oxidation of $\mathbf{1}$ to $\mathbf{1}^+$ remained constant. These CVs are typical of a “total catalysis” redox behavior involving a (co)-substrate-diffusion-controlled catalytic reaction (pre- peak), as well as a catalyst-diffusion-controlled process (second peak).^{9b, 10c, 17} To rationalize this behavior, bulk electrolysis of $\mathbf{1}$ was carried out in excess of 2,6-lutidine (8 equiv. vs. $\mathbf{1}$). $^1\text{H-NMR}$ analysis of the resulting products indicated that the methyl groups of the 2,6-lutidine were not oxidized (Fig. S7).

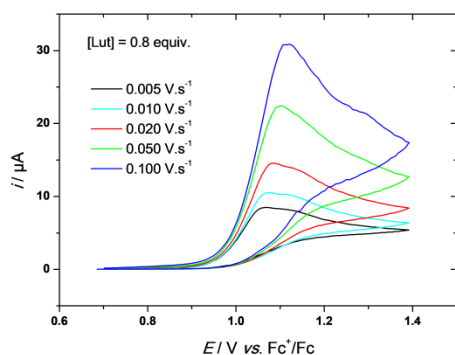
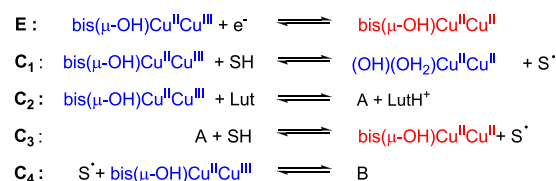


Fig.4 CVs of $\mathbf{1}$ (0.8 mM) with $[\text{Lut}] = 0.6$ mM at different scan rates; 0.1 M $\text{NBu}_4\text{ClO}_4/\text{CH}_3\text{CN}$ at 20°C under Ar.

Addition of water induced a slight increase of the catalytic current up to around 10 equiv. until to reach a plateau, consistent with the recovering of hydroxido bridges (Fig. S8). Hence, these results strongly suggest that acetonitrile acts as substrate for the electrocatalytic reaction in presence of base.

In order to further analyze this redox behavior, plots of $i_{\text{pa}}(2)$ vs. $[\text{Lut}]$ (from CVs displayed in Fig. 3) and $i_{\text{pa}}(2)$ vs. $v^{1/2}$ (from CVs displayed in Fig. 4), allowed the bounds of the total catalysis regime to be determined ($i_{\text{pa}}(2)$ is defined as the anodic peak current at $E_{\text{pa}}(2)$).^{9b} A straight-line variation was obtained from plots of $i_{\text{pa}}(2)$ vs. $v^{1/2}$ for $5 < v < 100$ $\text{mV}\cdot\text{s}^{-1}$ (Fig. S10B). Moreover, the $i_{\text{pa}}(2)$ vs. $[\text{Lut}]$ plot deviates from a straight-line at a 2,6-lutidine concentration greater than 1.5 equiv. (Fig. S10A). As the criteria for a total catalysis were fulfilled in the CVs displayed in Fig. 3, the number of electrons involved was extracted from the plot of pre-peak current against the square root of the scan rate¹⁷ (see ESI). The calculations indicated a mono- electronic process. Given this, a peak shift analysis of the data displayed in Fig. 4 was performed for the determination of the kinetics of the catalytic reaction (see ESI, Fig. S11). Noteworthy, the calculated rate constant value ($k_{\text{obs}} = 6 \times 10^4 \text{ M}^{-1}\cdot\text{s}^{-1}$) was significantly higher than that of the stoichiometric reaction of $\mathbf{1}^+$ with toluene H8 ($1.1 \text{ M}^{-1}\cdot\text{s}^{-1}$, see above).

To further investigate the effect of the base, voltammetric simulations were carried out according to an $\text{EC}_1\text{C}_2\text{C}_3\text{C}_4$ mechanism (Scheme 1, details in ESI). After electrochemical oxidation (step E), two chemical reactions are competing (C_1 and C_2): that of the electrogenerated $\text{Cu}^{\text{II}}\text{Cu}^{\text{III}}$ $\mathbf{1}^+$ species with the substrate SH (here $\text{SH} = \text{CH}_3\text{CN}$ as no toluene is present in this experiment) (step C_1) which probably yields a radical S^\bullet species together with a dicopper(II) hydroxido aqua complex, and that of $\mathbf{1}^+$ with 2,6-lutidine to form species \mathbf{A} (step C_2). Species \mathbf{A} then reacts with SH (step C_3) to regenerate the bis($\mu\text{-OH}$) Cu^{II}_2 species, according to a catalytic pathway. Finally the step C_4 was added to account for the reaction of S^\bullet with the bis($\mu\text{-OH}$) $\text{Cu}^{\text{II}}\text{Cu}^{\text{III}}$ species, making the oxidation peak at $E_{\text{pa}}(1)$ irreversible, as experimentally observed. A good match between the simulated and the experimental curves (Fig. S12) was obtained by considering the steps C_2 (deprotonation of $\mathbf{1}^+$) and C_3 (oxidation of the substrate) as very fast, in agreement with a “total catalysis” case. Best fits were found for rate

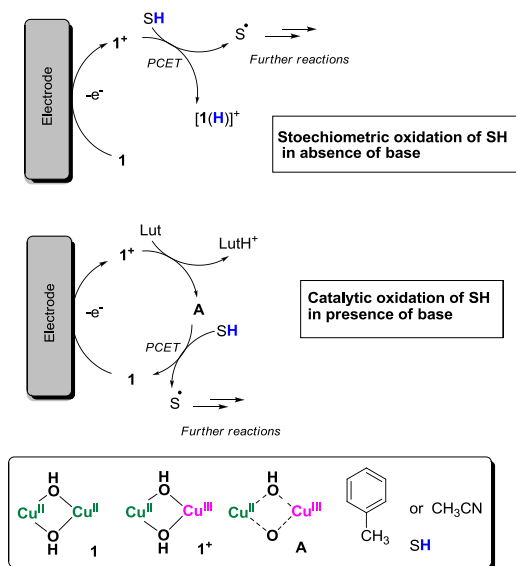


Scheme 1. EC₁C₂C₃C₄ proposed mechanism used for voltammetric simulations (details in ESI).

constant values of $k_f(\text{C}_2) = 7 \pm 1 \times 10^5$ and $k_f(\text{C}_3) = 10 \pm 1 \times 10^5 \text{ M}^{-1}\cdot\text{s}^{-1}$. These values are comparable with that determined from peak-shift analysis ($k_{\text{obs}} = 6 \times 10^4 \text{ M}^{-1}\cdot\text{s}^{-1}$).

These voltammetric studies clearly demonstrate that the addition of base (*i*) triggers the mechanistic pathway from a stoichiometric reaction to a catalytic one, and (*ii*) enhances by a four-order magnitude the rate constant of the oxidation of the C–H bond. Different active species, namely 1^+ and **A**, are involved for the stoichiometric and catalytic oxidation of the substrates, respectively (Scheme 2). Although the species **A** has not been isolated, we propose that deprotonation of 1^+ occurs on one of the bridging OH groups, leading to an oxido hydroxido Cu^{II}Cu^{III} species (**A**) (Scheme 2). Deprotonation of the μ -OH group is indeed more favored for 1^+ than **1**, because of the probable decrease of the pKa of the oxo/hydroxido group at the Cu(III)-Cu(II) redox state (vs. Cu(II)-Cu(II)).

Finally, the same catalytic experiments were performed with addition of toluene which did not induce any significant modification of the voltammetric response. However, bulk electrolysis of the toluene-based solution led to the formation of benzaldehyde, benzyl alcohol and benzylacetamide, although the yield in oxidized products from toluene is low as shown by GC analysis (see details in ESI and Fig. S13). Such a result is consistent with the fact that both toluene and acetonitrile display close BDE values (89.8 and 93 kcal·mol⁻¹ respectively) and can both be oxidized by species **A**.



Scheme 2. Electrochemical SH activation by **1** without or with 2,6-lutidine (Lut).

In summary, we have demonstrated that a Cu^{II}Cu^{III} species reacts with toluene in a single turnover reaction, functionalizing the aliphatic C–H bonds in the RDS. The addition of a base renders the system catalytic even without toluene suggesting that CH₃CN acts as a substrate. In this case, the observed rate constant determined to be $6 \times 10^4 \text{ M}^{-1}\cdot\text{s}^{-1}$ was refined through simulations to give a value of $7 \pm 1 \times 10^5 \text{ M}^{-1}\cdot\text{s}^{-1}$, and alludes to a possible oxido hydroxido Cu^{II}Cu^{III} (**A**) as the active species. It is in agreement with the previous proposal that (μ -O)(μ -

OH)Cu^{II}Cu^{III} cores can be active species for oxidation of methane to methanol.^{4a} To the best of our knowledge, this work is the first electrochemically copper-catalyzed C–H oxygenation and in addition operating in mild conditions. This proof of concept study demonstrates the oxidative reactivity of Cu^{II}Cu^{III} species towards exogenous substrates and has shed light on such high-valent species as new potent catalytic motifs in oxidative attack of strong sp³ C–H bonds. The electrochemical C-H activation described in this work appears to be selective as no aromatic C-H activation is observed. Furthermore with ethylbenzene as alternative substrate only the benzylic position is activated (see details in ESI and Fig S14). Future work will be focused on characterizing the transient active species responsible for C–H activation and optimizing this system, mainly by tuning the pK_a and redox potential of the complexes.¹⁸ This breakthrough should be further developed for expanding the scope of selective and sustainable oxidation reactions.

The authors gratefully acknowledge C. Costentin for fruitful discussion about this work. The French research agency is acknowledged for support (ANR-13-BSO7-0018) and ICMG FR 2607 (PCN-ICMG). This work has been partially supported by Labex ARCANE (ANR-11-LABX-0003-01) and CBH-EUR-GS (ANR-17-EURE-0003).

Conflicts of interest

There are no conflicts to declare.

Notes and references

1. X. Thang, X. Jia and Z. Huang, *Chem. Sci.*, 2018, **9**, 288.
2. a)A. E. Wendlandt, A. M. Suess and S. S. Stahl, *Angew. Chem. Int. Ed.*, 2011, **50**, 11062; b)S. E. Allen, R. R. Walvoord, R. Padilla-Salinas and M. C. Kozlowski, *Chem. Rev.*, 2013, **113**, 6234.
3. a)D. A. Quist, D. E. Diaz, J. J. Liu and K. D. Karlin, *J. Biol. Inorg. Chem.*, 2017, **22**, 253; b)C. E. Elwell, N. L. Gagnon, B. D. Neisen, D. Dhar, A. D. Spaeth, G. M. Yee and W. B. Tolman, *Chem. Rev.*, 2017, **117**, 2059; c)L. M. Mirica, X. Ottenwaelder and T. D. Stack, *Chem. Rev.*, 2004, **104**, 1013; d)S. Itoh, *Curr. Opin. Chem. Biol.*, 2006, **10**, 115; e)A. Ghazanfar, P. E. VanNatta, D. A. Ramirez, K. M. Light and M. T. Kieber-Emmons, *J. Am. Chem. Soc.*, 2017, **139**, 18448; f)J. Y. Lee and K. D. Karlin, *Curr. Opin. Chem. Biol.*, 2015, **25**, 184; g)C. Citek, S. Herres-Pawlis and T. D. P. Stack, *Acc. Chem. Res.*, 2015, **48**, 2424; h)K. V. N. Esguerra and J.-P. Lumb, *Synthesis*, 2019, **51**, 334; i)R. Trammell, K. Rajabimoghdam and I. Garcia-Bosch, *Chem. Rev.*, 2019, **119**, 2954.
4. a)Y. Shiota, G. Juhász and K. Yoshizawa, *Inorg. Chem.*, 2013, **52**, 7907; b)R. L. Lieberman and A. C. Rosenzweig, *Nature* 2005, **434**, 177–182.
5. a)M. R. Halvagar, P. V. Solntsev, H. Lim, B. Hedman, K. O. Hodgson, E. I. Solomon, C. J. Cramer and W. B. Tolman, *J. Am. Chem. Soc.*, 2014, **136**, 7269; b)A. Kochem, F. Gennarini, M. Yemloul, M. Orio, N. Le Poul, E. Rivière, M. Giorgi, B. Faure, Y. Le Mest, M. Réglie and A. J. Simaan, *ChemPlusChem*, 2017, **82**, 615; c)F. Gennarini, R. David, I. López, Y. Le Mest, M. Réglie, C. Belle, A. Thibon-Pourret, H. Jamet and N. Le Poul, *Inorg. Chem.*, 2017, **56**, 7707; d)A. Thibon-Pourret, F. Gennarini, R. David, J. A. Isaac, I. Lopez, G. Gellon, F. Molton, L. Wojcik, C. Philouze, D. Flot, Y. Le Mest, M. Réglie, N. Le Poul, H. Jamet and C. Belle, *Inorg. Chem.*, 2018, **57**, 12364.
6. a)T. C. Davenport and T. D. Tilley, *Angew. Chem. Int. Ed.*, 2011, **50**, 12205; b)T. C. Davenport, H. S. Ahn, M. S. Ziegler and T. D. Tilley, *Chem. Commun.*, 2014, **50**, 6326; c)T. C. Davenport and T. D. Tilley, *Dalton Trans.*, 2015, **44**, 12244.
7. J. A. Isaac, F. Gennarini, I. Lopez, A. Thibon-Pourret, R. David, G. Gellon, B. Gennaro, C. Philouze, F. Meyer, S. Demeshko, Y. Le Mest, M. Réglie, H. Jamet, N. Le Poul and C. Belle, *Inorg. Chem.*, 2016, **55**, 8263.
8. M. B. Robin and P. Day, *Adv. Inorg. Chem. Radiochem.*, 1968, **10**, 247.
9. a)M. L. Pegis, C. F. Wise, D. J. Martin and J. M. Mayer, *Chem. Rev.*, 2018, **118**, 2340; b)J.-M. Savéant, *Chem. Rev.*, 2008, **108**, 2348; c)C. Costentin, M. Robert and J.-M. Savéant, *Curr. Opin. Electrochem.*, 2017, **2**, 26; d)D. L. DuBois, *Inorg. Chem.*, 2014, **53**, 3935.
10. a)J.-M. Savéant, in *Elements of molecular and biomolecular electrochemistry: an electrochemical approach in electron transfer chemistry*, Wiley, Hoboken NJ . 2006; b)E. S. Rountree, B. D. McCarthy, T. T. Eisenhart and J. L. Dempsey, *Inorg. Chem.*, 2014, **53**, 9983; c)K. L. Lee, N. Elgrishi, B. Kandemir and J. L. Dempsey, *Nat. Rev. Chem.*, 2017, **1**, 1.
11. a)S. Berardi, S. Drouet, L. Francàs, C. Gimbert-Suriñach, M. Guttentag, C. Richmond, T. Stoll and A. Llobet, *Chem. Soc. Rev.*, 2014, **43**, 7501; b)X.-J. Su, C. Zheng, Q.-Q. Hu, H.-Y. Du, R.-Z. Liao and M.-T. Zhang, *Dalton Trans.*, 2018, **47**, 8670; c)S. Dey, B. Mondal, S. Chatterjee, A. Rana, S. Amanullah and A. Dey, *Nat. Rev. Chem.*, 2017, **1**, 98 ; d)R. Angamuthu, P. Byers, M. Lutz, A. L. Spek and E. Bouwman, *Science*, 2010, **327**, 313; e)X.-J. Su, M. Gao, L. Jiao, R.-Z. Liao, P. E. M. Siegbahn, J.-P. Cheng and M.-T. Zhang, *Angew. Chem. Int. Ed.*, 2015, **54**, 4909.
12. J. J. Warren, T. A. Tronic and J. M. Mayer, *Chem. Rev.*, 2010, **110**, 6961.
13. J. A. B. Satrio and L. K. Doraiswamy, *Chem. Eng. J.*, 2001, **82**, 43.
14. a)H. R. Lucas, L. Li, A. A. Narducci Sarjeant, M. A. Vance, E. I. Solomon and K. D. Karlin, *J. Am. Chem. Soc.*, 2009, **131**, 3230; b)C. Würtele, O. Sander, V. Lutz, T. Waitz, F. Tuzcek and S. Schindler, *J. Am. Chem. Soc.*, 2009, **131**, 7544.

15. a) C. Suspène, S. Brandes and R. Guilard, *Chem. Eur. J.*, 2010, **16**, 6352; b) C.-C. Liu, T.-S. Lin, S. I. Chan and C.-Y. Mou, *J. of Catalysis*, 2015, **322**, 139.
16. P. S. Engel, W.-K. Lee, G. E. Marschke and H. J. Shine, *J. Org. Chem*, 1987, **52**, 2813.
17. C. Costentin, D. G. Nocera and C. N. Brodsky, *Proc. Natl. Acad. Sci.*, 2017, **114**, 11303.
18. D. Dhar, G. M. Yee and W. B. Tolman, *Inorg. Chem.*, 2018, **57**, 9794.